

Mechanism of groundwater inrush hazard caused by solution mining in a multilayered rock salt mining area: A case study in Tongbai, China

Bin Zeng^{1*}, Tingting Shi², Zhihua Chen¹, Liu Xiang³, Shaopeng Xiang⁴, Mui Yang¹

¹. School of Environmental Studies, China University of Geosciences, Wuhan 430074, Hubei, P.R.China.

². Three Gorges Research Center for Geo-Hazard, Ministry of Education, Wuhan 430074, Hubei, P.R.China.

³. Department of Geological Engineering, Hubei Land Resources Vocational College. Wuhan 430074, P.R.China.

⁴. Hydrological Engineering Environment Technology Consulting Co. Ltd. Wuhan 430074, P.R.China.

***Corresponding author:** Bin Zeng, Ph.D.

Affiliation: School of Environmental Studies, China University of Geosciences.

Affiliation address: No. 388 Lumo Road, Wuhan, Hubei, 430074, P.R. China.

Email: zengbin_19@126.com. Tel: 86-27-67883473. Fax: 86-27-87436235.

1 **ABSTRACT**

2 The solution mining of salt mineral resources may contaminate groundwater and lead to water
3 inrush out of the ground due to brine leakage. ~~Taking~~ a serious groundwater inrush hazard in a large salt
4 mining area in Tongbai County, China, ~~as an example~~, this study mainly aims to analyze the source and
5 channel of the inrushing water. The mining area has three different types of ore beds including trona
6 (trisodium hydrogencarbonate dihydrate, also sodium sesquicarbonate dihydrate, with the formula
7 $\text{Na}_2\text{CO}_3 \cdot \text{NaHCO}_3 \cdot 2\text{H}_2\text{O}$, ~~is~~ a non-marine evaporite mineral), glauber (sodium sulphate, ~~is~~ the inorganic
8 compound with the formula Na_2SO_4 as well as several related hydrates) and gypsum (a soft sulphate
9 mineral composed of calcium sulphate dihydrate, with ~~the~~ chemical formula $\text{CaSO}_4 \cdot 2\text{H}_2\text{O}$). Based on
10 ~~the characterizing of~~ geological and hydrogeological conditions, hydrochemical data of the groundwater
11 at different points and depths were used to analyze the pollution source and pollutant component from
12 single or mixed brines by using physical-chemical reaction principle analysis and hydrogeochemical
13 simulation method. Finally, possible leakage brine conducting channel to the ground was discussed
14 from both geological and artificial aspects. The results reveal that the brine from the trona mine is the
15 major pollution source; there is a fissure zone ~~in the NW-SE direction~~ controlled by the geological
16 structure that provides the main channels for the leakage brine to flow into the aquifer around the water
17 inrush regions, ~~and a~~ large number of waste gypsum exploration boreholes ~~are~~ the channels that supply
18 the polluted groundwater inrush out of the ground. This research can offer a valuable reference for
19 avoiding and assessing groundwater inrush hazards in similar rock salt mining areas, which is
20 advantageous for both groundwater quality protection and public health.


21 1. Introduction

22 Solution mining is commonly used in salt mine exploitation, as salts are soluble in water. In this
23 method, high-pressure and -temperature water with low salinity is injected into a mineral deposit
24 through production wells to dissolve the mineral salts. After being drawn from the wells, the soluble salt
25 is purified and further processed. However, the high-pressure and -temperature water used in this
26 process not only dissolves minerals but also cause fractures in the strata, which usually results in
27 hazards such as brine leakage or groundwater inrush. In this situation, drinking groundwater for the
28 public is normally polluted following groundwater inrush, creating a hazard and threatening the health
29 of local residents.

30 Many scholars (Clark and Fritz, 1997; Liu et al., 2015; Wu et al., 2016) have studied groundwater
31 inrush hazards in both coal and metal mines, and some adopted methods are as follows: the use of water
32 level/temperature criterion (Yuan and Gui, 2005; Ma and Qian, 2014), stochastic simulation
33 (Fernandez-Galvez et al., 2007), numerical simulation (Liu et al., 2009; Kang et al., 2012; Shao et al.,
34 2013; Houben, et al., 2017), water chemical analysis (isotope analysis, water quality type correlation
35 analysis) (Robins, 2002; Fernandez et al., 2005; Hu et al., 2010; Cobbina et al., 2015; Lee et al., 2016;
36 LeDoux et al., 2016), multivariate statistics (discriminant analysis, clustering analysis) (Chen and Li,
37 2009; Lu, 2012), fractional advection dispersion equations (Ramadas et al., 2015) and nonlinear
38 analysis (fuzzy mathematics, grey correlation analysis, etc.) (Hao et al., 2010; Gao, 2012). However,
39 due to the particularity of the solution mining method and the complex chemical-physical reactions
40 during the high-pressure and -temperature mining process, researches regarding solution mining were
41 mainly focused on mining techniques (Jiang and Jiang, 2004; Kotwica, 2008; Namin et al., 2009),
42 mining cavity stability analysis and sinkhole problems (Staudtmeister and Rokahr, 1997; Bonetto et al.,
43 2008; Ezersky et al., 2009; Goldscheider and Bechtel, 2009; Closson and Abou Karaki, 2009; Vigna et

44 al., 2010; Frumkin et al., 2011; Ezersky and Frumkin, 2013; Qiu, 2011; Blachowski et al., 2014), and
45 geohazards particularly in karst areas due to human-induced underground caving (Waltham and Fookes
46 2003; Parise and Gunn 2007; Zhou and Beck 2011; Parise and Lollino 2011; Lollino et al., 2013;
47 Gutierrez et al., 2014; Parise et al., 2015), but rarely on source and channel analysis of inrush water in a
48 solution mining accident.

49 The study case of rock salt mining area is located in Tongbai County, Henan Province, China. This
50 mining area has the second largest trona reserves in the world, while its glauber salt reserves reach 45
51 million tons. Since trona and glauber salt were put into production in 1990 with single- and double-well
52 convection mining as the main producing method, five inrush points appeared in the town of Anpeng,
53 Tongbai County, from June 2011 to May 2013. Among these five inrush points, four (Y1~Y4) were
54 long-term (longer than 2 years) inrush points with stable discharge, while one (Y-5) was a sudden inrush
55 point (as shown in Fig. 1 and Fig. 2). Almost 200 m³ of mud and sediment erupted out of the ground at
56 the Y-5 point on 1 February 2013. The area of the inrush point was ~4 m²; the average water inflow was
57 20-30 m³/d while the greatest inflow reached 200 m³/d. The water inrush lasted for approximately three
58 months. During the Y-5 inrush accident, according to the field investigation, a trona production well
59 named “S02,” which is 200 m far from the inrush point, broke at a depth of 234 m and remained broken
60 for a long period of time. It was repaired on 15 March 2013. During the entire water inrush process, the
61 groundwater inrush led to a phenomenon of salinization at the house base of many villagers, and made
62 water in many residents’ wells no longer drinkable.

63 Since the groundwater inrush hazard involved a wide geographic area and the inrush source was 
64 quite hard to distinguish due to the multi-layer distribution of the different ore bodies and the
65 complexity of the inrush water component. Therefore, in order to put forward a targeted treatment
66 program to stop the water inrush as soon as possible, and mitigate the groundwater pollution in research

67 region, the source and channel of the inrush water were taken as the research emphasis in this study.
68 Furthermore, this research can provide a valuable reference for avoiding and assessing groundwater
69 inrush hazards in similar rock salt mining areas, which is advantageous for both groundwater quality
70 protection and public health.

71 **2. Geological and hydrogeological setting**

72 **2.1. Geological conditions**

73 The mining area is located in northwestern Tongbai County. The landscape is characterized by
74 hollows and ridges, with an elevation ranging from 140 to 200 m above sea level. The strata, lithology,
75 aquifer, and the position of different ore beds in the research area (Shi et al., 2013) are shown in Fig. 3.

76 According to geologic references and field investigation, in the northeastern mining area, a hidden
77 east-west oriented fault ~~is developed~~ at the bottom of the first segment of the Hetaoyuan Formation, and
78 another four, hidden, south-north oriented faults ~~are developed~~ at the bottom of the second segment of
79 the Hetaoyuan Formation. These five faults are outside the scope of trona mine, so they have little
80 effects on the ore bed. A few small-scale hidden faults ~~are developed~~ at the bottom of the third segment
81 of the Hetaoyuan Formation, although within the scope of the glauber salt mine, they have little effects
82 on the glauber salt ore bed which is distributed at the top of the first segment of Hetaoyuan Formation.
83 A hidden east-west oriented fault is developed at the bottom of the Liaozhuang Formation in the range
84 of the glauber salt mine, but it has little effects on the glauber salt mine because of its small scale.

85 **2.2. Hydrogeological conditions**

86 The groundwater in the mining area can be divided into pore water in the loose rock mass and
87 bedrock fissure water according to the lithology and hydrogeological features. In the upper part of the
88 Liaozhuang Formation, a mudstone interbedded with gypsum is considered a relative weak permeable
89 stratum especially under the condition of high-pressure and -temperature water injection during the

90 mining period. The shallow aquifer is unconsolidated pore water above this weak permeable stratum,
91 while the deep aquifer is a bedrock fissure beneath this weak permeable stratum.

92 The flow direction of the shallow groundwater is controlled by the regional terrain. Taking the
93 underground watershed as the boundary, the groundwater on the south side of the watershed is mainly
94 flowing from northeast to southwest with the Yanhong River as the drainage base , while the
95 groundwater on the north side of the watershed is mainly flowing from south to north with the Xia
96 River as the drainage base. The deep groundwater is in relatively closed burial conditions, with slow
97 velocity, and nearly the same flowing direction as the shallow groundwater. The water inflow of a single
98 well with poor water content is approximately 100 m³/d, while it can reach ~~from~~ 1000-2000 m³/d if it
99 has rich water content. The annual amplitude of the groundwater level is from 2 to 4 m, while the depth
100 is stable at 2.3-4 m. Residents in Anpeng use groundwater as their drinking water, which comes from
101 wells ~~and is from~~ the porous aquifer.

102 Gypsum mainly occurs ~~on~~ the top of the Liaozhuang Formation, glauber salt occurs in the third
103 member of the Hetaoyuan Formation, and the trona occurs at the bottom of the second member of the
104 Hetaoyuan Formation ~~as well as on top of the first member of the Hetaoyuan Formation~~ (Fig. 3). The
105 surrounding rocks of every mineral layer, including mudstone, shale, sandy conglomerate, psammitic
106 rock and dolomite, have sufficient thickness and good water-resistance. Therefore, the effect of
107 groundwater on the mineral deposit is minimal in the mining area.

108 ***2.3 Distribution and characteristics of the ore body***

109 The three ore bodies overlap in plane distribution, as shown in Fig. 4. The vertical distribution of
110 the ore bodies from deep-to-shallow is trona (buried depth: 1560.92-2929.53 m), glauber salt (buried
111 depth: 1003.66-1397.58 m) and gypsum (buried depth: 134-338 m). The trona and glauber salt bodies
112 are at least 250 m apart from each other vertically.

The trona has 11 horizontal layers, with an average thickness of 2.11 m. The chemical composition of trona is mainly NaHCO_3 (average of 77.06%) and Na_2CO_3 (average of 16.33%) (Wang, 1987). The glauber salt has 4 layers, with an average thickness of 8.93 m. The dip angle of the ore bed layer is less than 10° . The average mineral grade is 60.14%. The main composition of the glauber salt is Na_2SO_4 (>90%) with a small amount of NaCl .

3. Methods

Based on the field investigation results, the chemical ~~characteristic~~ analysis of the inrush water at different sites and time, analysis of the physical and chemical reaction principles for the different brines, ~~and~~ combined with the PHREEQC simulation method, the source of the inrush water was determined.

3.1. Sampling and testing

The five groundwater inrush points (Y1~Y5) and some shallow groundwater points (resident wells: SY1~SY6) near the accident site were chosen as groundwater quality sampling points, as shown in Fig. 4. Water from each point was sampled on 9 March 2013.

Water samples were filtered using a $0.45\ \mu\text{m}$ millipore filtration membrane in the field, and then filled with a polyethylene bottle which had been soaked in acid and washed with deionised water. Filtered water samples were acidified until ~~the~~ $\text{pH} < 2$ by addition of ultra-pure HNO_3 for the determination of cations; water samples for the determination of anions were not treated.

Elements tested in the laboratory included 26 cations (K^+ , Na^+ , Ca^{2+} , Mg^{2+} , Sr^{2+} , etc.) and 5 anions (F^- , Cl^- , NO_3^- , SO_4^{2-} , NO_2^-). The instrument used for the determination of cations was an inductively coupled plasma atomic emission spectrometer (Agilent ICP-OES 5100), ~~and the~~ minimum detection limit ~~was~~ 0.0001mg/L . The instrument used for the determination of anions was an ion chromatograph (ICS-1100), and the minimum detection limit was 0.001 mg/L . CO_3^{2-} and HCO_3^- were tested according to the “Groundwater quality test method: Determination of carbonate and bicarbonate by hydroxide

136 titration (DZ/T 0064.49-93),” and the minimum detection limit was 0.01 mg/L.

137 In addition, from March to April 2013, at the Y-5 and Y-3 points, three water quality automatic
138 recorders (Levellogger gold, Canada) were arranged for inrush water monitoring. Monitoring indicators
139 were temperature, water level and electrical conductivity. The purpose of the monitoring was to fully
140 understand the inrush water quality during the whole accident, especially in the process of well
141 reparation.

142 ***3.2. Analysis of the physical and chemical reaction principles in different brine mixing conditions***

143 During the accident, the leakage brine of the trona (2000 m below ground) or glauber salt (1000 m
144 below ground) might flow through the gypsum deposit (200-400 m below ground), which is comprised
145 primarily of CaSO_4 , and cause physical and chemical reactions while it inrushes out of the ground. Thus,
146 the formation of the chemistry component in inrush water might be from glauber brine, or trona brine,
147 or a mixture of the two brines, flowing through the gypsum layer accompanying physical and chemical
148 reactions. To provide the basis for further analysis of the inrush water source, the physical solubility of
149 the gypsum and the reaction when the glauber salt brine, trona brine, or a mixture of trona and glauber
150 salt brine flowing through the gypsum deposits were analyzed.

151 ***3.2.1. The physical solubility of gypsum (CaSO_4)***

152 Gypsum is slightly soluble; when in water, its acidity is apparent. Eq. (1) provides the dissolution
153 rate equation of gypsum in water:

$$154 \quad R_{\text{Gypsum}} = k_1 \times \frac{A_g}{V} \left(1 - \left(\frac{IAP}{K} \right)_{\text{Gypsum}} \right) \quad (1)$$

155 R_{Gypsum} : the dissolution rate of gypsum; k_1 : rate constant; A_g : the surface area of gypsum; V : the
156 liquid volume in contact with the gypsum surface; IAP : the product of ion activity; and K : ion solubility
157 product.

$\left(\frac{IAP}{K}\right)_{Gypsum}$ is affected by the temperature; thus, it is the same as R_{Gypsum} .

The solubility of gypsum in water reaches a maximum of 0.2097 g/100 g at 40°C. The solubility decreases when the temperature is below or above 40°C. The content of SO_4^{2-} and Ca^{2+} obtained by physical dissolution is very low.

3.2.2. Gypsum ($CaSO_4$) dissolved by glauber salt brine (Na_2SO_4)

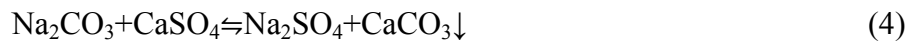
Equations (2) and (3) show the reactions of Na_2SO_4 and $CaSO_4$ with water.



Because of the common-ion effect, the solubility of the electrolyte will decrease when a strong electrolyte with the same ion is placed into an electrolyte-saturated solution. Thus, the solubility of gypsum will be reduced when glauber salt brine flows through and dissolves the gypsum deposits; the gypsum will be even harder to dissolve in this situation. Thus, if the glauber salt brine flows through the gypsum deposits, the brine characteristic would not apparently change.

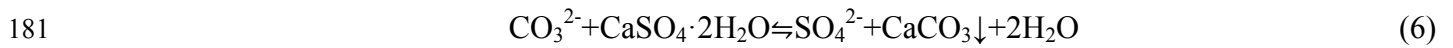
3.2.3. The reaction of trona brine or a mixture of trona and glauber salt brine with gypsum

The HCO_3^- and CO_3^{2-} contents in trona brine or in mixed brine are very high as is the solution alkalinity and pH. If the reaction kinetics is not taken into account, the pH has little influence on the dissolution of gypsum (Yang, 2003; Xu and Li, 2011). The reaction occurs when the brine with high concentrations of HCO_3^- and CO_3^{2-} flows through the gypsum deposits. The main chemical reactions are as follows:



In Eq. (4), $CaSO_4$ is slightly soluble, while $CaCO_3$ is insoluble. The reaction easily occurs when an

insoluble substance is produced by a slight soluble substance, and the ionic equation is as follows:



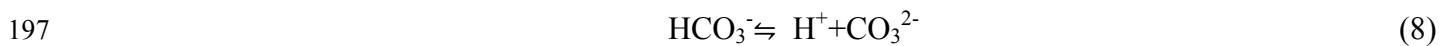
The Gibbs Free Energy (ΔG) is -22.7 kJ/mol under the standard state. When ΔG is negative, the reaction, which is endothermic, occurs freely. The reaction is faster at higher temperatures. Eq. (5) shows that ΔG is 2102 kJ/mol under the standard state. When ΔG is positive, the reaction will not freely occur.

Thus, the reaction shown in Eq. (5) will not occur, but the chemical reaction will still proceed as shown in Eq. (4), when trona brine or mixed brine flow through the gypsum deposits.

3.2.4. The carbonate equilibrium effect during the reaction of different brines

The carbonate equilibrium ~~that exists~~ in the trona brine or mixed brine is affected by pH. The carbonate in groundwater exists in three forms: free carbonic acid, bicarbonate and carbonic acid.

In the trona brine (pH>10), the concentration of HCO_3^- is 5-20 times that of the CO_3^{2-} concentration, and CO_3^{2-} in the brine is dominant in this case. When the trona brine flows through the gypsum, CaSO_4 reacts with CO_3^{2-} and CaCO_3 precipitates. If the concentration of CO_3^{2-} in the brine decreases, a reversible reaction will take place and drive the equilibrium to the right. Thus, the reverse reaction will occur when the trona brine flows through the gypsum as follows:



The circular reactions as shown in Eqs. (7) and (8) will occur when mixed brine flows through the gypsum because it has similar properties to the trona brine. Thus, taking the carbonate equilibrium effect into account, the concentrations of HCO_3^- and CO_3^{2-} will decrease, while SO_4^{2-} increases after CaCO_3 precipitates.

202 3.3. Simulation of groundwater inrush source

203 For further quantitative analysis of the inrush water source and component, the international
204 hydrological and geochemical simulation software PHREEQC was used to simulate the water-rock
205 interaction. The PHREEQC software was developed by the U.S. Geological Survey, and it is able to
206 calculate geochemical action within a temperature range of ~~from~~ 0~300 degrees (Wei, 2010).

207 Based on the deduction that the main water inrush source around Anpeng was trona leakage brine,
208 the simulation method PHREEQC was used and combined with the possible channel of inrush water to
209 establish a conceptual model ~~and then~~ hydrogeochemical simulation of the water-rock interaction was
210 conducted. Subsequently, the mixed ratio of inrush groundwater and shallow groundwater around
211 Anpeng were quantified, ~~which can~~ better verify the source of the inrush water.

212 3.3.1. Conceptual model

213 Around Anpeng, the trona leakage brine flowed through the specified mineral assemblages and
214 mixed with shallow groundwater in different proportions.

215 3.3.2. Initial data input

216 The parameters of the trona brine were taken from the enterprise's production testing data; ~~the~~
217 parameters of the shallow groundwater were taken from the same aquifer but outside the study area, and
218 can basically represent groundwater background values. The specific parameters are shown in Table 1.

219 3.3.3. Setting of stratum and mineral

220 The formations from the bottom to the top during the process of the leakage brine flowing into the
221 shallow groundwater and then flowing out of the ground were as follows: the third member of the
222 Hetaoyuan Formation of Paleogene, the Liaozhuang Formation and the Fenghuang Formation of
223 Neogene and Quaternary. To simplify the mining area, according to the thickness of the rock stratum
224 and the proportion of mineral composition, it can be assumed that the layer through which the trona

225 brine flowed contains Ca-montmorillonite, kaolinite, gypsum, potash feldspar and potash mica.

226 The main ingredients are as follows: Kaolinite: $\text{Al}_4[\text{Si}_4\text{O}_{10}](\text{OH})_8$; Gypsum: $\text{CaSO}_4 \cdot 2\text{H}_2\text{O}$;
227 Ca-montmorillonite: $(\text{Na}, \text{Ca})_{0.33}(\text{Al}, \text{Mg})_2[\text{Si}_4\text{O}_{10}](\text{OH})_2 \cdot n\text{H}_2\text{O}$; Dolomite: $\text{CaMg}(\text{CO}_3)_2$; Potash feldspar:
228 $\text{K}[\text{AlSi}_3\text{O}_8]$; Potash mica: aluminium silicate as K, Al, Mg, Fe and Li.

229 **4. Results and Discussion**

230 On 9 March 2013, in Anpeng, water samples from five groundwater inrush points and six
231 surrounding water quality monitoring points (resident well) were tested. The results of water chemical
232 composition are shown in Table 2, and the distribution of the sampling points is shown in Fig. 4.

233 According to the water quality analysis, the inrush brine had a relatively high salinity, with some
234 inrush water samples containing $\text{SO}_4\text{-Na}$ and some containing $\text{HCO}_3\text{-Na}$. The crystals mainly consisted
235 of NaSO_4 , Na_2CO_3 , and NaHCO_3 . The composition of the inrush water and the crystals was the same as
236 that of the high-concentrated ions in the trona brine (Na_2CO_3 , NaHCO_3 , etc.) and glauber salt brine
237 (Na_2SO_4).

238 **4.1. The source of the inrush water**

239 An automatic water quality recorder was set up at the Y5 inrush point on 4 March 2013. The
240 monitoring lasted from 5 March to 20 March 2013. Thus, the relationship between the inrush points and
241 the S02 well can be assessed according to the correlation of the changes between temperature/electrical
242 conductivity and the concentration of brine during the S02 production well reparation period (5 March
243 to 14 March 2013).

244 The production of glauber ceased during the investigation (2 March to 15 March 2013), so it could
245 be determined how the glauber mining affects the water inrush hazard based on a dynamic water quality
246 situation.

247 4.1.1. The source of inrush water at the Y-5 point

248 After successful reparation of the S02 well, the conductivity and temperature of the inrush water
249 decreased significantly. The CO_3^{2-} concentration remained at 0, the HCO_3^- concentration decreased to
250 500 meq/L, while the SO_4^{2-} concentration increased to 600 meq/L. Subsequently, the concentrations of
251 these three ions were in a state of dynamic balance. The analysis shows that the source of the inrush
252 water at the Y-5 point is closely related to the S02 trona well.

253 In order to ensure whether the glauber brine exists at this point as part of an inrush source, further
254 analysis was performed. The depth of the well rupture was 234 m; the gypsum deposit was developed to
255 this depth. While the leakage of the trona brine flowed through the gypsum deposit, reactions would
256 occur as shown in Eqs. (7) and (8).

257 According to the ion milliequivalent concentrations (Ca^{2+} : 0.61 meq/L; CO_3^{2-} : 905.3 meq/L; HCO_3^- :
258 1332.94 meq/L; Cl^- : 107.43 meq/L; and SO_4^{2-} : 267.89 meq/L) at the Y-5 point, the concentration of Ca^{2+}
259 was negligible compared to the other main ions. Only the reaction between CO_3^{2-} and CaSO_4 had to be
260 taken into account because of the large number of CO_3^{2-} , with fast velocity, the short contact time with
261 gypsum, and the high temperature. The reaction of CO_3^{2-} and CaSO_4 would take place at a ratio of 1:1
262 according to Eq. (7), and three types of inrush water sources could be assumed under this precondition
263 as follows:

264 (1) The inrush water source was only from the trona brine.

265 The CO_3^{2-} and CaSO_4 in the brine reacted at a ratio of 1:1, and the SO_4^{2-} concentration was equal
266 to the reacted γCO_3^{2-} content. Thus, the $\gamma\text{CO}_3^{2-}/\gamma\text{HCO}_3^-$ ratio in the trona brine was equal to the
267 $\gamma(\text{CO}_3^{2-}+\text{SO}_4^{2-})/\gamma\text{HCO}_3^-$ ratio in the inrush water. From this calculation, it could be seen that
268 $\gamma(\text{CO}_3^{2-}+\text{SO}_4^{2-})/\gamma\text{HCO}_3^-$ was equal to 0.88, while $\gamma\text{CO}_3^{2-}/\gamma\text{HCO}_3^-$ ranged between 0.86 and 1.26. The
269 content of $\gamma(\text{CO}_3^{2-}+\text{SO}_4^{2-})/\gamma\text{HCO}_3^-$ was similar to $\gamma\text{CO}_3^{2-}/\gamma\text{HCO}_3^-$; therefore, the source of the inrush

270 water was exclusively trona brine.

271 (2) The inrush water source was only from the glauber brine.

272 The $\gamma\text{SO}_4^{2-}/\gamma\text{HCO}_3^-$ ratio in the glauber brine was equal to 1237.8, compared to 0.19 in the inrush
273 water. Therefore, this assumption was incorrect because of the widely varying ratios.

274 (3) The inrush water source was from a mixed brine of glauber and trona.

275 Assuming that the contribution ratio of the glauber brine was X and that of the trona brine was Y ,
276 then $1237.8 \times X + (0.86 \sim 1.26) \times Y = 0.88$. This equation showed that when the contribution ratio of
277 the trona brine was equal to 1, the contribution ratio of the glauber brine was equal to 1.6×10^{-5} , which is
278 too small that can be ignored.

279 Thus, it could be confirmed that the water inrush source at Y-5 was exclusively the leakage of trona
280 brine from the broken S02 well.

281 4.1.2. The sources of inrush water at the Y-4, Y-3, Y-2, and Y-1 points

282 The inrush water quantity and the dynamic variation of the concentration of SO_4^{2-} and HCO_3^- at
283 points Y1-Y4 were not obvious when the S02 well was under repair and all the glauber wells were shut
284 down (from 2 to 15 March). This result shows that the sources of these water inrush points were not due
285 to the underground mining activities of the glauber brine or the rupture of the S02 well, but because of
286 the brine leakage from other trona wells.

287 4.1.3. Components and mixed proportions of the inrush water

288 The PHREEQC simulation conditions were assumed to be as follows: (1) the trona brine did not
289 mix with shallow groundwater after flowing through the mineral layer; or (2) the trona brine mixed with
290 shallow groundwater in a ratio of 1:2, 1:10, 1:100, 1:200, 1:500, 1:1000 and 1:5000 after flowing
291 through the mineral layer. The simulation results are shown in Table 3



292 Table 3 shows that when the trona brine flowed through the stratum and shallow groundwater, the

concentrations of Na^+ , Cl^- and SO_4^{2-} decreased while the HCO_3^- concentration increased with increasing proportion of shallow groundwater. The Ca^{2+} concentration decreased at first and then increased.

The ion concentrations at Y-5, except for SO_4^{2-} , were similar to the ion concentrations in the trona brine. However, at the same time, the HCO_3^- concentration was nearly 0 meq/L. When the trona brine flowed through the layer, it would react rapidly and pour out of the ground directly because of the fast velocity of the inrush water at Y-5. Meanwhile, the trona brine was not continuously provided in the simulation. Thus, the concentration of HCO_3^- would be near to the concentration of trona brine in reality. Therefore, the trona brine must have a rapid inrush, almost not mixing with shallow groundwater.

The PHREEQC simulation results show that: 1) the water inrush source of Y-5 was the trona brine almost all from the ruptured S02 well; 2) the water inrush source of Y-3 was a mixture of trona brine and groundwater in a ratio of 1:10~1:100; and 3) the water inrush sources of Y-4, Y-2 and Y-1 were a mixture of trona brine and groundwater under the ratio of 1:200.

4.2. The channel of the inrush water

4.2.1. Reasons for the brine leakage

Trona is produced by either a single well or double/multiple well convection mining method that is water-soluble mining method (Lin, 1987). The main mining unit consists of a salt cavity and production well. Thus, the instability of the salt cavity and the rupture of the production well are the main possible reasons for brine leakage.

(1) Analysis of salt cavity stability

The possibility of salt cavity collapse: Trona is distributed at the bottom of the second member of the Hetaoyuan Formation and in the upper part of the first member of the Hetaoyuan Formation, with dolomite strata developed in the roof and floor. The thick and hard surrounding rock structure determined that the cavity is produced by hydrofracture but it is hard to fill with large-scale fractured



316 channels and can remain intact and stable.

317 The development of a roof fracture: When a mineral is under exploitation, the surrounding rock in
318 the cavity is under pressure from the inner brine. This pressure is equal to the sum of the water injection
319 pressure and the water column pressure in the production well. The water injection pressure of the trona
320 production well is approximately 10-20 MPa, while the 1560.92-2929.53 m (mineral buried depth)
321 water column pressure is approximately 15.3-28.71 MPa. Thus, the greatest water pressure on the
322 surrounding rock in the cavity is 48.71 MPa. The main lithology of the surrounding rock is dolomite
323 ~~that is~~ 500 m in thickness and 142.66 MPa in compressive strength, which is nearly 3 times that of the
324 greatest possible water pressure. Therefore, large-scale fractures in the surrounding rock of the trona
325 mineral would be difficult to develop under the effect of sustained water pressure.

326 (2) Analysis of production well rupture

327 The phenomenon of brine leakage caused by the S02 well rupture in Anpeng indicates that
328 production well damage is an important cause of brine leakage. The depth of the S02 well rupture is 234
329 m underground, i.e. in the gypsum deposit, which is strongly hygroscopic. The pressure caused by the
330 water swelling is approximately 0.15 MPa (Li and Zhou, 1996), which may damage the production well
331 and induce brine leakage. The high concentration of SO_4^{2-} (>250 mg/L) generated by the reaction of
332 leakage brine and gypsum can also corrode the production well and lead to groundwater inrush.

333 4.2.2. Analysis of water-conducting channel

334 According to our analysis, the most probable reason for brine leakage in trona is production well
335 rupture. The leaking brine will flow along the water-conducting channel into the shallow aquifer and
336 even pour out of the ground. However, the geological structure in the mining area shows no
337 water-conducting fault development. Thus, the water-conducting channel, that the leakage brine flows

338 along, is probably a fissure or artificial channel.

Structural fissure is the main type of fissure that occurs in groundwater inrush hazards when using the solution mining method. The structural fissure is determined by the maximum horizontal principal stress, which is controlled by the tectonic stress field in the mining area. The connection direction of the S02 well and the other water inrush points is NW-SE, ~~which is~~ the same as that of the structural fissure zone development direction. This ~~result~~ indicates that the main water-conducting channel in Anpeng is controlled by the structural fissure zone.

The inrush points in Anpeng are all at the abandoned gypsum exploitation wells, which were not closed properly. Thus, high-pressure cavity water or leakage brine can flow along the structural fissure zone, finally connect with these wells, and then pour out of the ground through boreholes. Therefore, the abandoned gypsum exploitation wells are the main channels through which the shallow polluted groundwater flowed out of the ground, as shown in Fig. 5.

5. Conclusions

This study aimed to investigate the source and channel of the inrush water in a multilayer rock salt mining area. To achieve the set objectives, an analysis of geological and hydrogeological conditions, an analysis of physical and chemical reaction principles of different brines, the PHREEQC simulation method, and an analysis of geological and artificial reasons for the conducting channel where leakage brine flowed from the damage depth out to the ground were combined ~~as the study methodology~~.

Long-term solution mining with high-pressure and -temperature water not only dissolves minerals but also may cause rupture of strata and damage of the production well, which usually results in brine leakage or groundwater inrush. Geological and hydrogeological conditions are the basis which determines the total risk of the groundwater inrush hazard. Physical and chemical reaction principle analysis of different brines and hydrogeochemical simulation of water-rock interaction in different assumed conditions using the PHREEQC simulation method can ~~not only~~ determine the exact source of

362 the leakage brine ~~but also~~ identify the mixed proportion of inrush water while the leakage brine flows
363 through the mineral layer ~~in different way~~. Other than geological reasons, mining techniques such as
364 pressure control of injection water and groundwater quality monitoring of exploitation wells may also
365 determine the risk of a groundwater inrush hazard in a multilayer rock salt mining area.

366 **Acknowledgements**

367 This work was partially supported by the Fundamental Research Funds for the Central Universities,
368 China University of Geosciences (Wuhan) [Grant Numbers: CUGL100219].

369 **Author Contributions**

370 Bin Zeng and Tingting Shi contributed to data analysis and manuscript writing; Zhihua Chen
371 proposed the main structure of this study; Liu Xiang and Mui Yang designed and performed the
372 experiments; and Shaopeng Xiang performed the PHREEQC simulation. All the authors read and
373 approved the final manuscript.

374 **Conflicts of Interest**

375 The authors declare that they have no conflict of interest.

376

377 **References**

- 378 Blachowski, J., Milczarek, W. and Stefaniak, P.: Deformation information system for facilitating
379 studies of mining-ground deformations, development, and applications, Nat. Hazards Earth
380 Syst. Sci., 14, 1677-1689, 2014
- 381 Bonetto, S., Fiorucci, A., Fornaro, M. and Vigna, B.: Subsidence hazards connected to quarrying
382 activities in a karst area: the case of the Moncalvo sinkhole event (Piedmont, NW Italy),
383 Estonian J. Earth Sci., 57, 125-134, 2008
- 384 Chen, H. J. and Li, X. Bi.: Studies of water source determination method of mine water inrush
385 based on Bayes' multi-group stepwise discriminant analysis theory, Rock and Soil Mechanics.,
386 30, 3655-3659, 2009.
- 387 Clark, I. D. and Fritz, P.: Environmental isotopes in hydrogeology, Lewis Publishers, New York,
388 USA, 35-37, 1997.
- 389 Closson, D. and Abou Karaki, N.: Salt karst and tectonics: sinkholes development along tension
390 cracks between parallel strike-slip faults-, Dead Sea-, Jordan. Earth Surface Processes and
391 Landforms., 1408-1421, 2009
- 392 Cobbina, S.J., Duwiejuah, A.B., Quansah, R., Obiri, S. and Bakobie, Noel.: Comparative
393 Assessment of Heavy Metals in Drinking Water Sources in Two Small-Scale Mining
394 Communities in Northern Ghana, Int. J. Environ. Res. Public Health., 12, 10620-10634,
395 2015.
- 396 Ezersky, M., Legchenko, A., Camerlynck, C. and Al-Zoubi, A.: Identification of sinkhole
397 development mechanism based on a combined geophysical study in Nahal Hever South area
398 (Dead Sea coast of Israel). Environmental Geology., 58, 1123-1141, 2009
- 399 Ezersky, M. and Frumkin, A.: Fault - Dissolution front relations and the Dead Sea sinkhole

problem. *Geomorphology.*, 201, 35-44, 2013

Fernandez, I., Olias, M., Ceron, J.C. and De la Rosa, J.: Application of lead stable isotopes to the Guadiamar Aquifer study after the mine tailings spill in Aznalcollar (SW Spain), *Environ Geol.*, 47, 197-204, 2005.

Fernandez-Galvez, J., Barahona, E., Iriarte, A. and Mingorance, M.D.: A simple methodology for the evaluation of groundwater pollution risks, *Sci Total Environ.*, 378, 67-70, 2007.

Frumkin, A., Ezersky, M., Al-Zoubi, A., Akkawi, E. and Abueladas, A.-R.: The Dead Sea sinkhole hazard: Geophysical assessment of salt dissolution and collapse. *Geomorphology.*, 134, 102-117, 2011

Goldscheider, N. and Bechtel, T.D.: The housing crises from underground – damage to a historic town by geothermal drillings through anhydrite, Staufen, Germany. *Hydrogeology Journal.*, 17, 491-493, 2009

Gao, W.D.: Application of Entropy Fuzzy Discriminating methods in Distinguishing Mine Bursting Water Source, *Mining Safety & Environmental Protection.*, 39, 22-24, 2012.

Gutierrez, F., Parise, M., De, Waele, J. and Jourde, H.: A review on natural and human-induced geohazards and impacts in karst. *Earth Science Reviews.*, 138, 61-88, 2014

Hao, B.B., Li C. and Wang C.H.: Application of grey correlation degree in the identification of sources of mine water bursting, *China Coal.*, 36, 20-22, 2010.

Hu, W.W., Ma, Z.Y., Cao, H.D., Liu, F., Li, T. and Dou, H.P.: Application of Isotope and Hydrogeochemical Methods in Distinguishing Mine Bursting Water Source, *Journal of Earth Sciences and Environment.*, 32, 268-271, 2010.

Houben, G.J., Sitnikova, M.A. and Post, V.E.A.: Terrestrial sedimentary pyrites as a potential source of trace metal release to groundwater – A case study from the Emsland, Germany, *Appl.*

423 Geochem., 76, 99-111, 2017.

424 Jiang, R.Z. and Jiang T.X.: Present Development and Prospecting of Hydraulic Fracturing
425 Technology, Oil Drilling & Production Technology., 26, 52-57, 2004.

426 Kang, X.B., Hu, X.W. and Xie, H.Q.: Numerical simulation on the influence of the groundwater
427 flow field during tunneling, Advanced Materials Research., pp. 1230-1233, 2012.

428 Kotwica, K.: Scenarios of technological development of roadways mining in polish coal mines
429 conditions, Gospod Surowcami Min., 24, 139-152, 2008.

430 Lee, H., Choi, Y., Suh, J. and Lee, S.H.: Mapping Copper and Lead Concentrations at Abandoned
431 Mine Areas Using Element Analysis Data from ICP–AES and Portable XRF Instruments: A
432 Comparative Study, Int. J. Environ. Res. Public Health., 13, 384, 2016.

433 LeDoux, T.M., Szynekiewicz, A. and Faiia, A.M.: Chemical and isotope compositions of
434 shallowgroundwater in areas impacted by hydraulic fracturing and surface mining in the
435 Central Appalachian Basin, Eastern United States, Appl. Geochem., 71, 73-85, 2016.

436 Lin, Y.X.: The History of Science & Technology of well salt in China, Sichuan Science and
437 Technology Pres, Chengdu, 1987.

438 Li, D.D. and Zhou, Z.A.: Possibility of corrosion failure of concrete shaftwall due to water
439 infiltration, Journal of China Coal Society., 21, 158-163, 1996.

440 Liu, H., Yang, T., Zhu, W. and Yu, Q.: Numerical analysis of the process of water inrush from the
441 12th coal floor FANGEZHUANG coal mine in China, Controlling Seismic Hazard and
442 Sustainable Development of Deep Mines: 7th International Symposium on ROCKBURST and
443 Seismicity in Mines (RASIM7)., 1&2, 1381-1386, 2009.

444 Liu, R.Z., Liu, J., Zhang, Z.J., Borthwick, A. and Zhang, K.: Accidental Water Pollution Risk
445 Analysis of Mine Tailings Ponds in Guanting Reservoir Watershed, Zhangjiakou City, China,

Int. J. Environ. Res. Public Health., 12, 15269-15284, 2015.

Lollino, P., Martimucci, V. and Parise, M.: Geological survey and numerical modeling of the potential failure mechanisms of underground caves. *Geosystem Engineering*-, 16, 100-112, 2013

Lu, J.T.: Recognizing of Mine Water Inrush Sources Based on Principal Components Analysis and Fisher Discrimination Analysis Method, *China Safety Science Journal*-, 22, 109-115, 2012.

Ma, L. and Qian, J.Z.: An approach for quickly identifying water-inrush source of mine based on GIS and groundwater chemistry and temperature, *Coal Geology & Exploration*-, 42, 49-53, 2014.

Namin, F. S., Shahriar K., Bascetin A. and Ghodsypour S.H.: Practical applications from decision-making techniques for selection of suitable mining method in Iran, *Gospod Surowcami Min.*, 25, 57-77, 2009.

Parise, M., and Gunn, J.: Natural and anthropogenic hazards in karst areas: Recognition, Analysis and Mitigation. *Geol. Soc. London, sp. publ.* 279, 2007

Parise, M. and Lollino, P.: A preliminary analysis of failure mechanisms in karst and man-made underground caves in Southern Italy. *Geomorphology*-, 134, 132-143, 2011

Parise, M., Closson, D., Gutierrez, F. and Stevanovic, Z.: Anticipating and managing engineering problems in the complex karst environment. *Environmental Earth Sciences*-, 74, 7823-7835, DOI :10.1007/s12665-015-4647-5, 2015

Qiu, Z.Y.: Mechanism analysis of surface collapse in the area of solution salt mining, *Journal of Safety Science and Technology*-, 7, 27-31, 2011.

Ramadas, M., Ojha, R. and Govindaraju, R.S.: Current and Future Challenges in Groundwater. II: Water Quality Modeling, *J. Hydrol. Eng.*, 13, 132-140, 2015.

- Robins, N.S.: Groundwater quality in Scotland: major ion chemistry of the key groundwater bodies, Sci Total Environ., 294, 41-56, 2002.
- Shao, A.J., Huang, Y. and Meng, Q.X.: Numerical Simulation on Water Invasion of Coal Mine, Applied Mechanics and Materials-, pp-1112-1117, 2013.
- Shi, T.T., Chen, Z.H. and Luo, Z.H.: Mechanism of groundwater bursting in a deep rock salt mine region: a case study of the Anpeng trona and glauber salt mines, China, Environ Earth Sci., 68, 229-239, 2013.
- Staudtmeister, K. and Rokahr, R.B.: Rock Mechanical Design of Storage Caverns For Natural Gas in Rock Salt Mass, Rock Mech&Min.Sci., 34, 3-4, 1997.
- Vigna, B., Fiorucci, A., Banzato, C., Forti, P. and De Waele, J.: Hypogene gypsum karst and sinkhole formation at Moncalvo (Asti, Italy). Z. Geomorphol., 54, 285-308, 2010
- Wang, J.M.: A Preliminary Study on the Characteristics and Conditions of forming Anpeng Trona deposits, Petrol Explor Dev., 5, 93-99, 1987.
- Waltham, AC. And Fookes, PG.: Engineering classification of karst ground conditions. Quarterly Journal of Engineering Geology and Hydrogeology-, 36, 101-118, 2003
- Wei, Y.N.: Research and Application of Hydro-geochemical Simulation, Journal of Water Resources and Water Engineering-, 21, 58-61, 2010.
- Wu, Q., Li, B. and Chen, Y.: Vulnerability Assessment of Groundwater Inrush from Underlying Aquifers Based on Variable Weight Model and its Application, Water Resour Manag., 30, 3331-3345, 2016.
- Xu, H. and Li, H.S.: Study on CaSO_4 crystallization process and its influential factors, Industrial Water Treatment-, 5, 67-69, 2011.
- Yang, Y.H.: Gypsum mineral dissolution kinetics, M.D. thesis, China University of Geosciences,

492 Wuhan, China, 2003.

493 Yuan, W.H. and Gui, H.R.: The Characteristics of Geothermal Temperature and Its Application in
494 Distinguishing the Source of Water in Ren Lou Mine, Journal of Anhui University of Science
495 and Technology (Natural Science)., 25, 9-11, 2005.

496 Zhou, W. and Beck, BF.: Engineering issues on karst. In: P. van Beynen (Ed), Karst Management.

497 Springer, Dordrecht, pp. 9-45, 2011

Figure captions

Fig. 1. One of the long-term (longer than 2 years) groundwater inrush points with stable discharge (Y-3).

Fig. 2. The sudden groundwater inrush point (Y-5). The high-temperature inrush groundwater was being pumped after the ground was broken.

Fig. 3. Information about strata, lithology, aquifers, and buried positions of each ore bed in the mining area.

Fig. 4. Sketch map of hydrogeological conditions and the distribution of groundwater inrush points in the mining area.




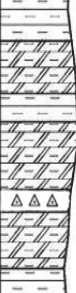

Fig. 5. Schematic diagram of the source and channel of the groundwater inrush hazard in the multilayered rock salt mining area in Tongbai County.



Fig.1



Fig.2

Stratigraphy				Thickness (m)	Lithologic profile	Petrographic description	Minerals	Aquifer
System	Series	Formation	Member					
Quaternary								
Neogene	Oligocene	Fenghuang zhen		0-290		Alternating layers of sandy conglomerate and sandy clay		Shallow aquifer
Paleogene	Eocene	Liaozhuang		500-634		Upper part: mudstones are interbedded with gypsum Lower part: alternating layers of mudstone and sandy conglomerate	Gypsum	Weak permeable stratum
			Third segment	400-500		Mudstone with interlayers of sandy conglomerate, as well as thin layers of shale, muddy dolomite and glauber salt	Glauber	Deep aquifer
		Hetaoyuan	Second segment	700-800		Mudstone is interlayered with muddy dolomite and dolomite, as well as small amounts of trona	Trona	
			First segment	1100-1700		Mudstone, muddy dolomite, dolomite, shale and siltstone	Trona	






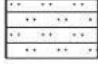
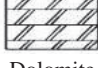
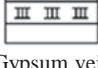
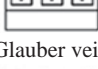
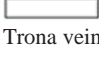
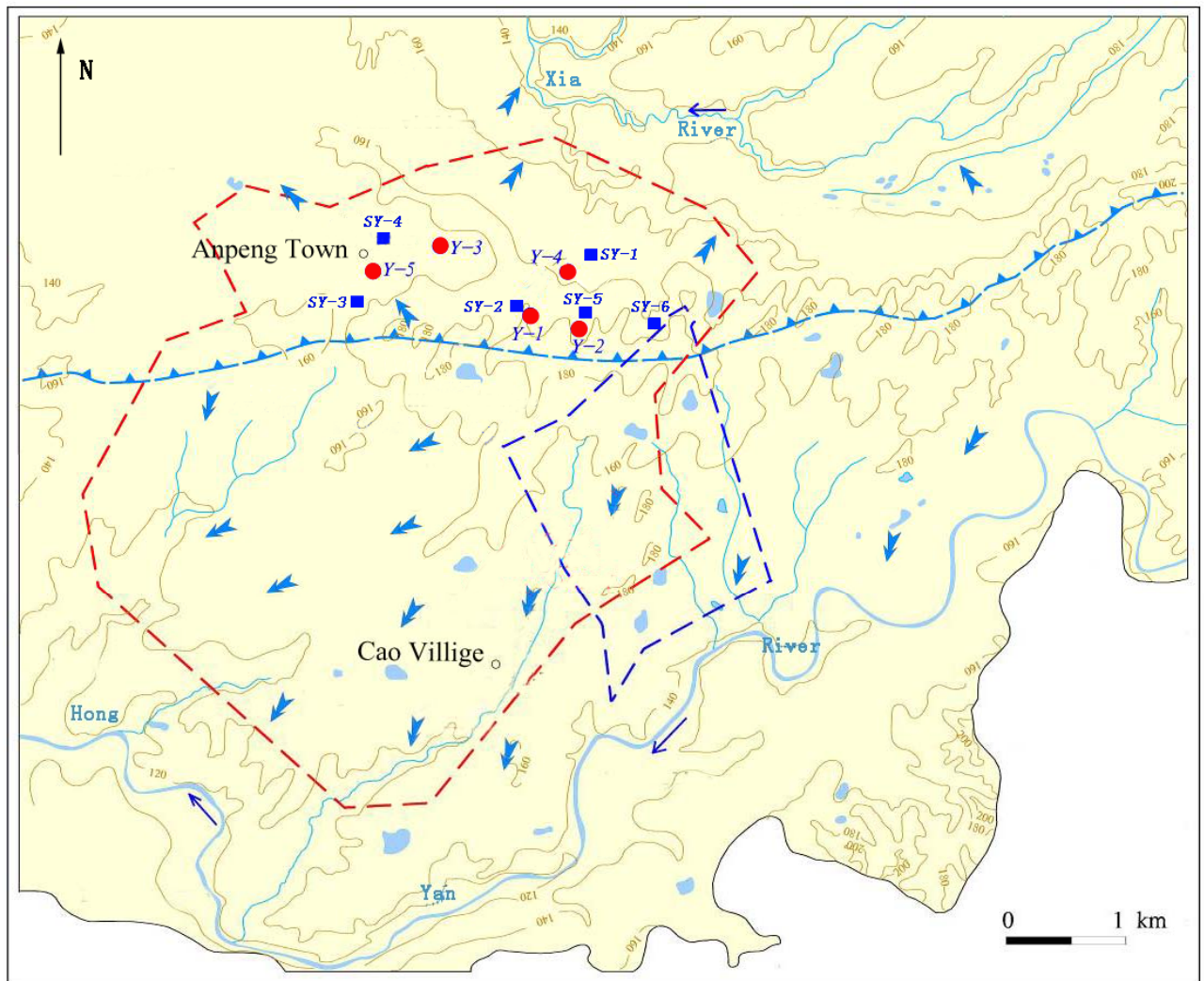
Legend	
	Sandy conglomerate
	Sandy clay
	Mudstone
	Muddy
	Shale
	Siltstone
	Dolomite
	Gypsum vein
	Glauber vein
	Trona vein

Fig.3





- | | | |
|----------------------------|--------------------------------|-------------------------------|
| Quaternary pore water | The area of trona mine | The area of glauber salt mine |
| Contour and elevation | Drainage divide of groundwater | Rivers and lakes |
| Groundwater flow direction | Groundwater intrush points | Resident well points |

Fig.4

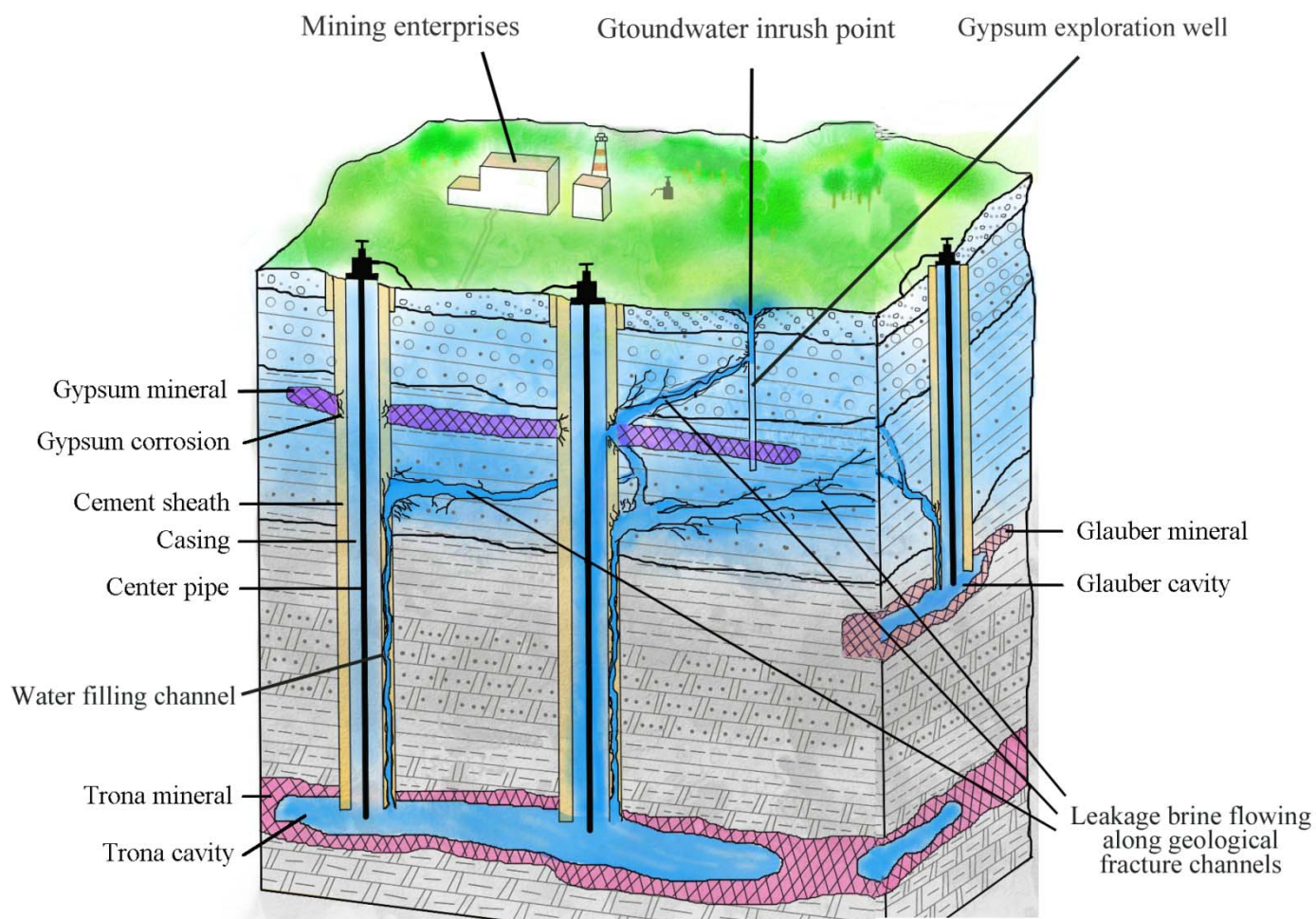


Fig.5

Table 1 Initial data of trona brine and background value of groundwater for the PHREEQC simulation

Type	Temperature (° C)	pH	Na ⁺	Ca ²⁺	Mg ²⁺	Cl ⁻	SO ₄ ²⁻	HCO ₃ ⁻	CO ₃ ²⁻
						(mg/L)			
Trona brine	70.00	10.80	85880.00	5.00	1.00	3819.00	206.00	104721.00	4565.00
Background value of groundwater	14.10	7.50	38.76	67.10	23.88	12.46	39.31	386.87	0.00

Table 2 Chemical composition of groundwater from the inrush hazard points and surrounding resident wells

Source	Point	Na ⁺	Ca ²⁺	Mg ²⁺	Cl ⁻	SO ₄ ²⁻	HCO ₃ ⁻	CO ₃ ²⁻	Salinity	Depth
(mg/L)										(m)
Groundwater from inrush hazard points	Y-1	447.30	91.20	74.68	171.18	278.55	1488.89	0.00	1807.35	330.55 ~ 430.20
	Y-2	524.50	89.34	75.32	153.97	298.88	1525.00	0.00	1904.51	
	Y-3	1132.00	146.60	158.30	125.56	4296.44	1012.93	0.00	6365.37	
	Y-4	322.12	98.67	123.88	210.78	346.55	1122.77	0.00	1663.38	
	Y-5	50300.00	12.23	53.21	3813.80	12858.63	81309.15	27159.00	107692.40	
Groundwater from resident wells around the inrush points	SY-1	46.28	76.76	17.29	64.30	14.58	319.03	0.00	378.73	10.00
	SY-2	28.37	98.02	27.46	26.16	10.38	453.84	0.00	417.31	
	SY-3	43.14	46.20	14.42	31.02	117.12	319.03	0.00	316.26	
	SY-4	118.53	278.40	72.30	425.23	175.96	568.52	0.00	1354.68	
	SY-5	31.67	95.51	19.22	53.93	22.59	351.97	0.00	398.90	
	SY-6	36.77	68.82	19.60	18.51	21.55	340.38	0.00	335.43	

Table 3 Simulation results for a mixed proportion of inrush trona brine using the PHREEQC method

Conditions	Mixed proportion with shallow groundwater	Na ⁺	Ca ²⁺	Cl ⁻	SO ₄ ²⁻	HCO ₃ ⁻
				(mg/L)		
Trona brine unmixed or mixed with different proportion of shallow groundwater after flowing through the mineral layer (simulation results)	Unmixing	87147.00	301.08	3880.15	68659.20	5.06
	1:1	48093.00	280.00	2145.62	37900.80	9.39
	1:2	33235.00	184.72	1485.68	26188.80	13.97
	1:10	9586.40	148.28	436.30	7561.92	57.95
	1:100	1098.25	90.40	141.63	873.89	306.34
	1:200	571.78	69.60	118.56	459.17	382.17
	1:500	252.77	68.32	104.60	207.84	453.66
	1:1000	144.81	67.52	99.94	105.12	481.60
Water quality test results in five water inrush hazard points	Y-1	447.30	91.20	171.18	276.55	1488.89
	Y-2	524.50	89.34	153.97	298.88	1525.00
	Y-3	1132.00	146.60	125.56	4296.44	1012.93
	Y-4	322.12	98.67	210.78	346.55	1122.77
	Y-5	50300.00	12.23	3813.80	12858.63	81309.15